

A mathematical study of the narrowband lambda sensor characteristics for lean and rich operation

ARTICLE INFO

Air-fuel ratio measurement is essential for efficient combustion and emission control in internal combustion engines. This study presents a mathematical model for the voltage response of narrowband zirconia lambda sensors, commonly used in older vehicles. These sensors, while cost-effective, are limited by their narrow operating range and strong temperature sensitivity – especially under rich mixture conditions. Using the Nernst equation, the study models the sensor voltage as a function of oxygen partial pressure. The sensor's heating element was experimentally characterized, and its resistance-temperature relationship was accurately described using a Rational5 function. A modified form of the Nernst equation enabled voltage-to-AFR conversion across a wide mixture spectrum. Data analysis confirmed that in lean conditions, the voltage response is nearly linear and largely unaffected by temperature, enabling accurate closed-loop control. In contrast, rich mixtures produced highly non-linear and temperature-dependent behavior, making interpretation more complex. To address this, an Arrhenius-based model was successfully applied to the rich-side response, significantly improving accuracy after temperature compensation. The model was implemented and tested on a Ford EEC V ECU with a Ford 302 GT40P engine running on LPG. Modifications to the controller allowed stable closed-loop operation up to $\lambda = 1.35$ using only a narrowband sensor. These results show that with proper modeling and calibration, narrowband lambda sensors can effectively monitor lean mixtures and offer limited utility in rich conditions. This opens new possibilities for retrofitting legacy engine systems without expensive hardware upgrades. Further research is needed to enhance rich-side precision and dynamic temperature correction.

Received: 17 June 2025

Revised: 7 July 2025

Accepted: 22 July 2025

Available online: 16 November 2025

Key words: *lambda, sensor, lean, burning, engine*This is an open access article under the CC BY license (<http://creativecommons.org/licenses/by/4.0/>)

1. Introduction

The measurement of the air-fuel ratio (AFR) is crucial for the proper operation of an internal combustion engine and the minimization of pollutant emissions. Both wide-band and narrowband lambda sensors play a key role in this process. The most commonly used solution in older vehicles is the zirconia narrowband sensor, which, despite its limited measurement range and slower response time, provides sufficient accuracy under typical operating conditions [14]. The operating principle of the lambda sensor is based on the electrochemical potential difference resulting from the unequal oxygen concentration on both sides of the oxide membrane. The mathematical description of this phenomenon follows directly from the Nernst equation [13], and its precise application in interpreting the lambda sensor voltage requires consideration of factors such as temperature, partial pressure, and the resistance characteristics of the heater [4, 2].

Technical and patent literature highlights significant challenges in interpreting the sensor signal in the range of extremely lean and rich mixtures, where the variability of oxygen partial pressure can span several orders of magnitude [1, 12]. For rich mixtures, the sensor signal is highly unstable and strongly dependent on temperature [8, 13], which limits its practical use in precise control systems. In parallel, alternative technologies such as titanium sensors or semiconductor cells with much higher thermal resistance and a broader measurement range are being developed [4, 8]; however, their application remains costly. Attempts to extend the durability and effectiveness of conventional

zirconia sensors have included the use of CFD simulations [2] and modifications to engine controller algorithms [14].

Modern approaches employ mathematical and numerical methods to model the real-time response behavior of the lambda sensor [13, 7], and also seek to establish relationships describing its characteristics as a function of partial pressure and temperature. At the same time, advanced ignition systems, such as microwave multipoint systems, are being developed, enabling operation with extremely lean mixtures – up to $\lambda = 2$ [9].

Current research places significant emphasis on maintaining an optimal air-fuel mixture over the widest possible range of engine loads and rotational speeds. This is especially important due to the strong correlation between AFR and mixture homogeneity in relation to the level of harmful emissions produced by the internal combustion engine. Additionally, alternatives such as gasoline blends with other hydrocarbons are being explored to reduce emissions [6, 15].

The aim of this article is to develop a consistent mathematical model describing the voltage characteristics of a narrowband lambda sensor across the full AFR range, with a division into operating conditions for lean and rich mixtures, while accounting for the influence of temperature and the heater resistance relationship. The conclusions drawn from the conducted research may contribute to more effective use of classic sensors in modern fuel mixture control systems and the retrofitting of older systems. Additionally, the ability to extend the operating range of a narrowband lambda sensor beyond the stoichiometric point ($\lambda = 1$) would enable improved calibration and adaptation of

engines with lambda-based control systems to operate on alternative fuels such as LPG, LNG, or ethanol – without the need for system reconstruction or the installation of additional devices. This could lead to increased efficiency and power output of vehicles running on alternative fuels, without sacrificing fuel economy. Such a solution would be feasible if the engine’s Powertrain Control Module (PCM) could be configured with different PI controller parameters for the lambda sensor response, tailored to various engine operating points – such as load, rotational speed, temperature, and others. This would allow lean mixture operation under high-load conditions, and fuel mixture leaning during low-load operation or in moments when high torque is not required. With the expansion of the control algorithm, more precise and broader emission control would become achievable. At present, in systems based on narrowband sensors, the engine controller only switches between predefined values for rich and lean conditions. Accurate signal interpretation would allow for control similar to that of wideband sensors. The relationship between emission levels and lambda values is presented in Fig. 1.

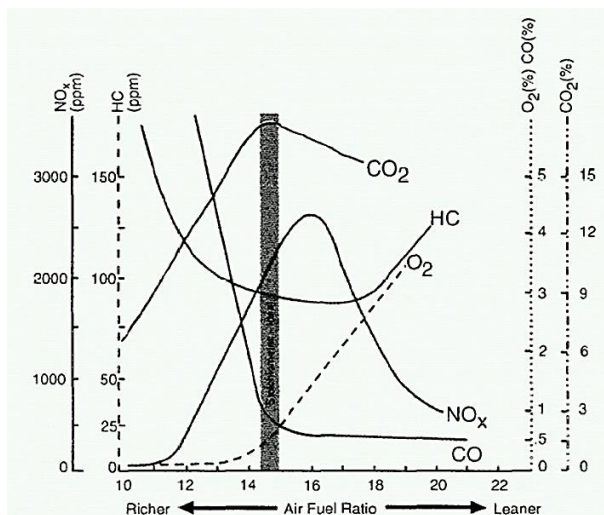


Fig. 1. AFR vs emissions [10]

2. Materials and methods

The experiment measuring the resistance of the heater in the sensor depending on its temperature was carried out on a classic zirconia lambda sensor. A planar sensor was not selected due to the fact that, in older vehicles, and for economic reasons, narrowband zirconia lambda sensors were more commonly used. Although they respond more slowly than titanium sensors, they are fully sufficient for less demanding applications, such as in everyday-use vehicles. A type K thermocouple was used to measure the temperature of the sensor. A temperature of up to 1000 °C was achieved by supplying the lambda sensor with up to 30 V from a laboratory power supply. The data analysis and calculations were carried out using OriginLab and Excel software. Likewise, all mathematical functions were determined using OriginLab. Initial formula transformations, including the Nernst equation, were performed in an OldSchool manner on paper. The identification of function formulas describing the experimental curves was done using fitting functions in OriginLab. Initial fitting parameters were se-

lected randomly, and then, using an algorithm with a fitting condition, values of the function variables were found that ensured the best fit to the plotted data. The choice of the initial fitting functions was based on the experimenter’s experience. Subsequent functions were verified in alphabetical order.

3. Basic calculations and description

The most important equation describing the operation of a lambda sensor is the Nernst equation. This equation defines the equilibrium potential of an electrode. In relation to the lambda sensor, the Nernst equation defines the voltage across the sensor’s electrodes depending on the difference in partial pressure between the exhaust system and the surrounding environment. More precisely, it is the partial pressure of oxygen that is crucial, as the sensor measures the difference in oxygen partial pressure. Air, serving as a reference value, is supplied to the lambda sensor through the signal wire. A vacuum of up to 1 bar can occur in this wire. For this reason, it is prohibited to solder the lambda sensor’s signal wires leading to its connector. Similarly, the use of products such as WD-40 or Contact Cleaner to clean the connectors of lambda sensors is also forbidden. Doing so may clog the capillaries in the signal wire, which can lead to the reversal of the voltage generated by the lambda sensor. As a result, a lean mixture may produce readings close to 1 V, while a rich mixture may cause the sensor to generate a voltage close to 0 V. A cross-section of the lambda sensor is shown in Fig. 2.

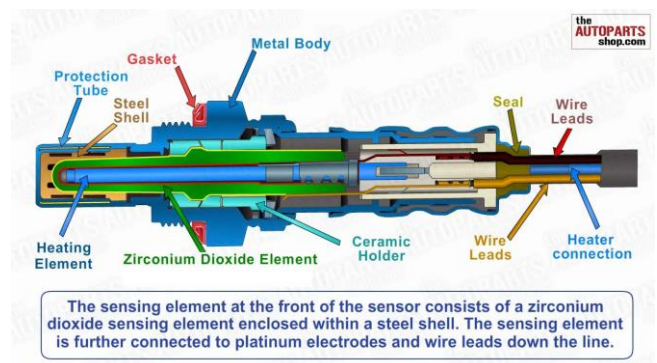


Fig. 2. Lambda sensor construction [5]

On the left side, the external shield is visible, designed to protect the cell from mechanical damage and from direct exposure to unburned fuel components. This is particularly important because large amounts of unburned fuel can cause the lambda sensor to indicate a falsely lean mixture. Just behind the protective element is the main electrode, which houses a heating element inside. Depending on the sensor model and its installation location, heaters with power ratings ranging from 3 to 24 W are used. The lowest-power heaters are typically found in planar sensors installed directly in the exhaust manifold. The purpose of the heater is to bring the sensor up to its operating temperature around 500°C as quickly as possible. Rapid heating allows the control system to switch to closed-loop mode, enabling fuel injection to be regulated based on feedback from the lambda sensor. This significantly reduces the emission of harmful substances. The zirconia electrode is mounted in a ce-

ramic holder, which is housed inside a metal tube. A real image of the sensor, both external and in cross-section, is shown in Fig. 3.



Fig. 3. Lambda sensor [11]

The Nernst equation for the lambda sensor takes the following form:

$$U = \frac{RT}{nF} \cdot \ln\left[\frac{P_a}{P_e}\right] \quad (1)$$

where: U – Lambda sensor output voltage, R – gas constant, T – temperature of the sensor/exhaust gases, n – electrons involved in the reaction = 4, F – Faraday constant, Pa – partial pressure of O₂ in the atmosphere, Pe – partial pressure of O₂ in the exhaust system.

The first issue encountered when attempting to identify the relationship with respect to lambda is the extremely different partial pressure values between the rich and lean sides of the lambda sensor's operation. In the case of the rich side, values can reach as low as 10 to the power of minus 23, whereas on the lean side, they can reach values up to the power of 3. Lambda 1 was adopted as the reference point. Another problem arises regarding the resistance of the sensor's heater. The equation clearly shows the influence of temperature on the voltage readings. Unfortunately, the full linearity of the resistance-to-temperature relationship is a fiction. To make matters worse, the equation does not define a relationship with lambda. For this reason, in order to use the equation in a control system, it becomes necessary to derive a formula describing the same voltage-generation relationship for lambda in terms of the difference in partial pressure.

To achieve this, a basic transformation of the equation was undertaken. An additional variable, k, was introduced to represent the term RT/nF. After transformations, the equation took the following form.

$$e^{(-U/k+\ln(P_a))} = P_e \quad (2)$$

$$e^{\ln(P_e)} = P_e \quad (3)$$

Having the equation transformed in this way and using tables that define the relationship between lambda and partial pressure, it became possible to attempt to identify consistent mathematical relationships and to verify whether the derived relationships are applicable.

4. Results

The first test of the correctness of the calculations was to verify whether the graph plotted using the derived equation is a logarithmic function. A test temperature of 750

degrees Celsius was assumed. Due to the very large difference in the ranges of partial pressures, correction coefficients for the lean side, rich side, and stoichiometry were applied to properly plot the curve. These coefficients indicate to the algorithm whether the system is operating on the lean or rich side. This makes it possible to filter out noise in the value ranges close to lambda 1, where the lambda sensor graph becomes almost a vertical line. The plot test confirmed that the function is indeed logarithmic. The shape of the curve is shown in Fig. 4. A total of 42 points were used to generate the graph.

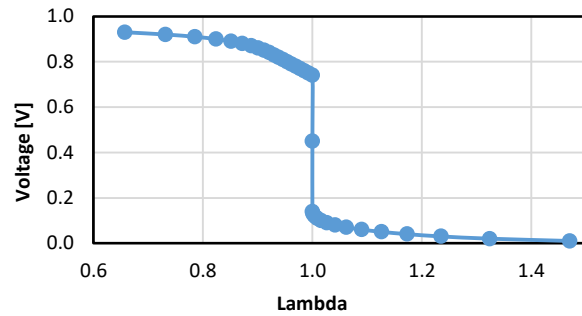


Fig. 4. Lambda vs voltage

The graph is identical to those found in textbooks. Across a very wide voltage range, the indicated air-fuel mixture remains at lambda = 1. Only at the extreme ends of the voltage scale does the lambda sensor indicate values deviating from the stoichiometric point. For rich mixtures, the voltage range is approximately 0.7 V to 0.95 V. On the lean side, the values range from around 0.15 V down to nearly 0 V. Another limitation is the 8-bit analog-to-digital converter, which is typically used in systems equipped with a narrowband lambda sensor.

The correct shape of the graph allows for further data processing. The next step was to plot and attempt to identify a function describing the relationship between the heater resistance and temperature, in order to enable compensation of the lambda sensor readings on both the lean and rich sides for a given, momentary operating temperature. The recorded measurements are presented in Fig. 5.

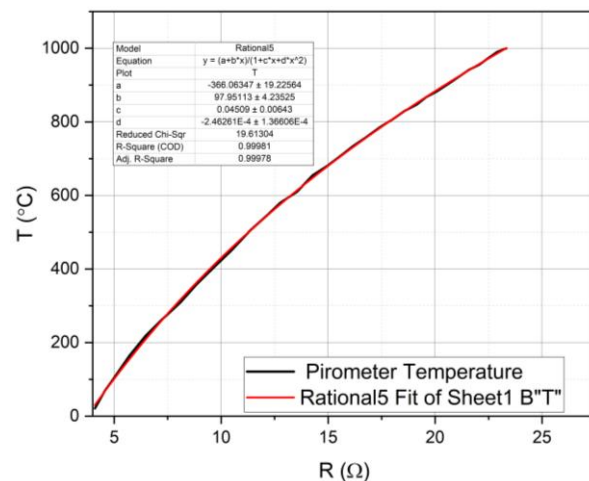


Fig. 5. Temperature vs resistance of lambda sensor heater

It was observed that the highest degree of fit is provided by the Rational5 function with appropriately selected coefficients, as shown in the graph.

The fitting function is plotted with a red line; subsequently, the relationship between lambda and the partial pressure difference was verified across the full spectrum from a lean mixture to a rich mixture. The results are presented in Fig. 6.

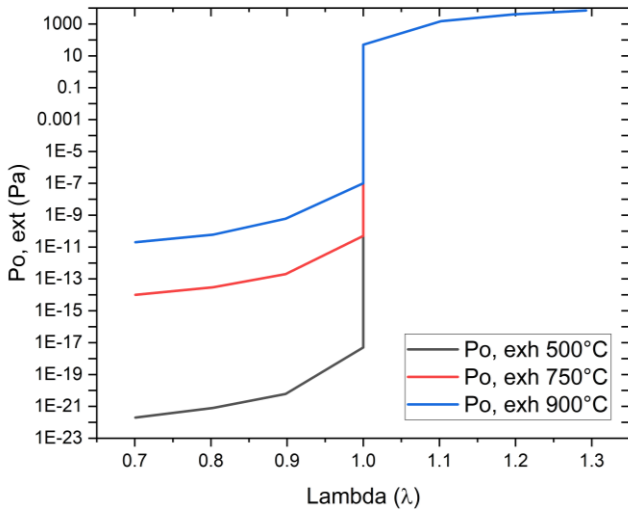


Fig. 6. Lambda vs partial pressure

The relationships were verified for the three temperatures indicated in the graph. A significant influence of temperature on the lambda sensor readings was detected on the rich side. This influence is so substantial that it greatly hinders the precise reading of rich mixtures using a narrowband sensor. For this reason, the first, more detailed calculations were carried out on the lean side. Initial results indicated a low influence of temperature on lean-side readings. More precise calculations were then performed, revealing an almost negligible impact of temperature on the sensor's readings on the lean side. This is illustrated in Fig. 7.

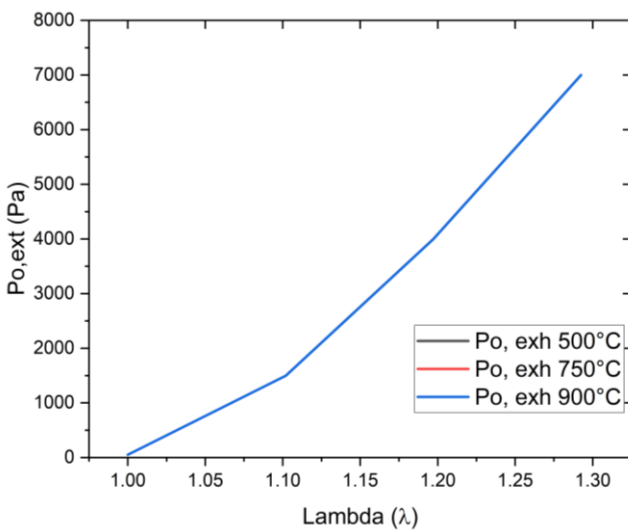


Fig. 7. Lean side of lambda sensor temperature dependence

The graphs for each temperature overlap. To better illustrate the full scope of the issue regarding the reading of lean and rich mixtures using a narrowband sensor, a graph was plotted where the y-axis represents lambda, and the x-axis indicates the difference in partial pressure as measured by the lambda sensor. The result is presented in Fig. 8.

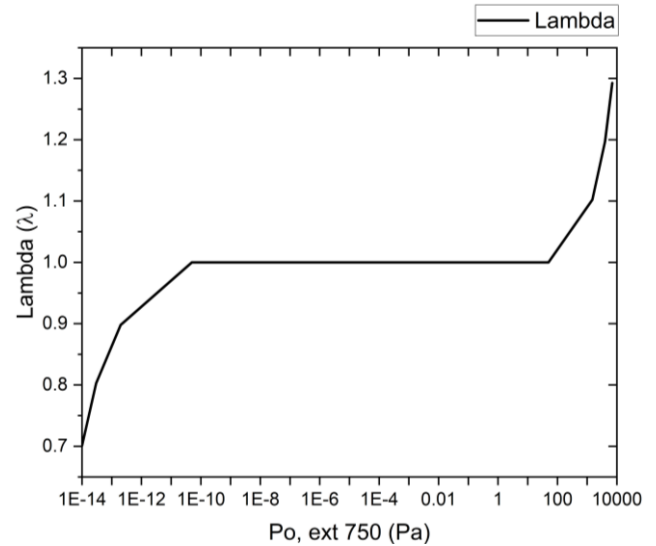


Fig. 8. Lambda vs partial pressure at 750 deg C

An important aspect is to pay close attention to the scale of the x-axis.

A closer look at the lean side of the lambda sensor readings revealed a nearly linear characteristic. For this reason, an attempt was made to determine the coefficients for the basic Rational5 function. The attempt was successful. The result is presented in Fig. 9.

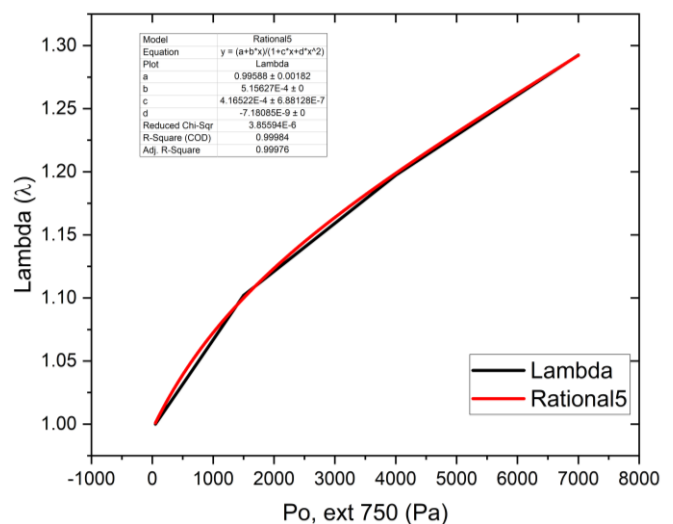


Fig. 9. Lean side of lambda sensor

This means that precise reading and control of the unit in closed-loop mode for lean mixtures is possible using a narrowband lambda sensor. The identified relationship was provisionally implemented for controlling the Ford EEC V system and a 1998 Ford 302 engine. Stable operation of the closed-loop correction system was achieved up

to the limits of stable engine operation on LPG fuel. For idle conditions, a lambda value of approximately 1.35 was reached. The controller's bias algorithm was modified to enforce only minimal voltage changes on the sensor, thereby eliminating large mixture swings. Due to the preliminary nature of this implementation, further in-depth research is required in this area, which is beyond the scope of this article. Subsequently, an attempt was made to find a function describing the lambda sensor readings on the rich side. Unfortunately, standard functions did not yield satisfactory results. However, a similarity was observed between the operating principle of the Nernst equation and the voltage generation mechanism in the lambda sensor cell, which is related to activation energy. The Arrhenius model, commonly used in semiconductor technology, turned out to be highly relevant. The similarity was not coincidental; the model very accurately describes the behavior of the sensor cell for rich mixtures. This is presented in Fig. 10.

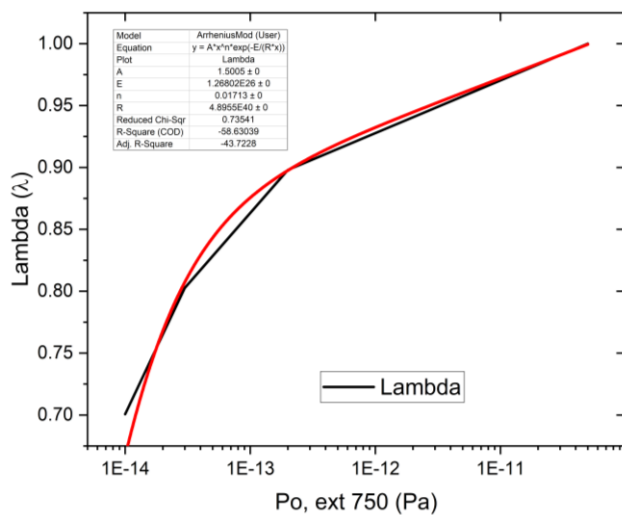


Fig. 10. Rich side of the lambda sensor

It can be observed that despite the large variation in partial pressures, it was possible to plot a curve based on the Arrhenius model. The greatest inaccuracy in the fit is seen

at a lambda value of 0.85. Above lambda 0.88, the fit is virtually perfect. The quality of the fit indicates the potential for practical application in a vehicle. After determining the coefficient values for the Arrhenius model and performing the temperature correction procedure, a complete relationship was developed, suitable for implementation in an engine control unit.

4. Summary and conclusion

The calculations, transformations, and tests performed using the narrowband sensor indicated the possibility of extending its application to include measurements in both lean and rich mixture ranges. However, measurements in the rich mixture range are associated with greater error and require more precise readings or a control system capable of maintaining a constant temperature in the lambda sensor. The downside of a system that maintains constant temperature is its inability to sustain that temperature under very high engine loads, which are typically the conditions where mixture enrichment occurs. The strong temperature dependency and very small partial pressure delta values on the rich side, combined with production variations among lambda sensors, raise doubts about achieving a reading accuracy for rich mixtures better than 10%. The situation is different on the lean side. Both the calculations and preliminary on-engine tests with the Ford 302 GT40P engine indicate proper sensor operation and the ability to accurately read lean mixture values. After algorithm adjustments, the Ford EEC V control system was able to operate correctly in closed-loop mode up to a lambda value of 1.35. The main modification to the control algorithm that was necessary for proper operation on the lean side was the adjustment of the bias and delay time. The control system is based on a PI (Proportional-Integral) controller. The bias and delay parameters are, in effect, indirect representations of the PI controller's parameters. Changes in their values affect overshoot, the functioning of the OBD II diagnostic system, and the rate of signal rise within the controller.

Further research is required to fully validate the algorithm's reliability. This, however, was beyond the scope of the present study.

Nomenclature

ADC	analog to digital converter	EEC	electric engine control
AFR	air to fuel ratio	LPG	liquid petroleum gas
CFD	computational fluid dynamics	PI	proportional-integral

Bibliography

- [1] Aravind S, Ragupathi P, Kumar DS, Vignesh G. A numerical investigation of automotive lambda sensor to improve the life span of the sensor using CFD. IOP Conf Ser Mater Sci Eng. 2020;923(1). <https://doi.org/10.1088/1757-899X/923/1/012003>
- [2] Bosch Engineering GmbH, Lambda Sensor LSU 4.9 data-sheet. 51865867 en, 1, 26. Aug. 2025
- [3] Collings N, Harris JA, Glover K. Estimating IC engine exhaust gas lambda and oxygen from the response of a universal exhaust gas oxygen sensor. Meas Sci Technol. 2013;24(9):095101. <https://doi.org/10.1088/0957-0233/24/9/095101>
- [4] Hills B. United States Patent Preparing Fire-Fighting Concentration US 4,464,267 1984;(19).
- [5] How Oxygen Sensor Works – Automotive Systems <https://youtu.be/F13aD1qJrEg?si=5diBaIOApx8ogVcH> (accessed on 10.06.2025).
- [6] Jakliński P, Czarnigowski J, Ścisłowski KJ. Study of the effect of ignition crank angle and mixture composition on the performance of a spark-ignition engine fueled with ethanol. Combustion Engines. 2024;197(2):56-63. <https://doi.org/10.19206/CE-174888>

- [7] Klett S, Piesche M, Heinzelmann S, Weyl H, Wiedenmann H, Schneider U et al. Numerical and experimental analysis of the momentum and heat transfer in exhaust gas sensors. SAE Technical Paper 2005-01-0037. 2005. <https://doi.org/10.4271/2005-01-0037>
- [8] Moos R, Izu N, Rettig F, Reiß S, Shin W, Matinfara I. Resistive oxygen gas sensors for harsh environments. Sensors. 2011;11(4):3439-3465. <https://doi.org/10.3390/s110403439>
- [9] Nishiyama A, Ikeda Y, Serizawa T. Lean limit expansion up to lambda 2 by multi-point microwave discharge igniter. 2018;247-260. Ignition Systems for Gasoline Engines: 4th International Conference December 6–7, 2018, Berlin. <https://doi.org/10.5445/IR/1000088587>
- [10] Run Lean Emissions Ecco modder forum thread <https://ecomodder.com/forum/showthread.php/run-lean-emissions-36327.html> (accessed on 10.06.2025)
- [11] Sensing the adequate mixture – the Bosch Lambda Sensor <https://www.bosch.com/stories/40-years-of-bosch-lambda-sensor/> (accessed on 10.06.2025).
- [12] Tang H, Prasad K, Sanjinés R, Lévy F. TiO₂ anatase thin films as gas sensors. Sensors and Actuators, B: Chemical. 1995. [https://doi.org/10.1016/0925-4005\(94\)01559-Z](https://doi.org/10.1016/0925-4005(94)01559-Z)
- [13] Toema M. Physics-based characterization of lambda sensor output to control emissions from natural gas fueled engines. An Abstract of a Disertation, Kansas State University, 2010.
- [14] Tutunea D, Dumitru I, Stănciuc-Oță OV. Overview of the use of oxygen sensors in automotive applications. IOP Conf Ser Mater Sci Eng. 2024;1303(1):012014. <https://doi.org/10.1088/1757-899X/1303/1/012014>
- [15] Urbański B, Przybyła G, Brodziński Ł, Savitskaya M. Reducing emissions of harmful substances in rally cars. Combustion Engines. 2024;197(2):132-8. <https://doi.org/10.19206/CE-181525>

Adam Kamiński, MEng. – Faculty of Mechanical Engineering, Wrocław University of Science and Technology, Poland.
e-mail: adam.kaminski@pwr.edu.pl

